CHIN. PHYS. LETT. Vol. 37, No. 12 (2020) 124203

Extreme Ultraviolet Frequency Comb with More than 100 μW Average Power below 100 nm

Jin Zhang(张津)[1,2], Lin-Qiang Hua(华林强)[1,2*], Zhong Chen(陈忠)[1,2], Mu-Feng Zhu(朱穆峰)[1,2], Cheng Gong(龚成)[1,2], and Xiao-Jun Liu(柳晓军)[1,2*]

[1]*State Key Laboratory of Magnetic Resonance and Atomic and Molecular Physics, Innovation Academy for Precision Measurement Science and Technology, Chinese Academy of Sciences, Wuhan 430071, China*
[2]*University of Chinese Academy of Sciences, Beijing 100049, China*

(Received 25 August 2020; accepted 9 October 2020; published online 8 December 2020)

Extreme ultraviolet (XUV) frequency comb is a powerful tool in precision measurement. It also brings many new opportunities to the field of strong field physics since high harmonic generation related phenomena can be studied with high repetition rate. We demonstrate the generation of an XUV frequency comb with the aid of intra-cavity high harmonic generation process. The setup is driven by a high power infrared frequency comb, and an average power of 4.5 kW is reached in the femtosecond enhancement cavity. With Xe gas as the working media, harmonics up to the 19th order are observed. Power measurement indicates that as much as 115.9 μW (1.3 mW) are generated at ∼94 nm (∼148 nm). The shortest wavelength we can reach is ∼55 nm. The coherence of the generated light is tested with an optical-heterodyne-based measurement of the third harmonic. The resulted line width is ∼3 Hz. In addition, with this system, we also observe a strong suppression of below threshold harmonics from O_2 compared to that from Xe. These results suggest that the current system is ready for precision spectroscopic measurements with few-electron atomic and molecular systems in XUV region as well as the study of strong field physics with an unprecedented 100 MHz repetition rate.

PACS: 42.60.Da, 42.65.Ky, 42.65.Re DOI: 10.1088/0256-307X/37/12/124203

As a new tool invented around 2005,[1,2] extreme ultraviolet (XUV) frequency comb has advanced impressively[3−17] and brought many new opportunities to the field of precision measurement[8,12,17] as well as strong field physics.[4,13,18] One typical example is the precision spectroscopic measurement of few-electron atomic and molecular systems, such as the $1S$–$2S$ transitions in He, He^+, Li^+, etc.,[19−25] with the aim of testing bound state quantum electrodynamics (QED) theory with high precision. Since these transitions lie in the XUV spectral region, for quite a long time, they are not accessible due to the lack of appropriate narrow bandwidth lasers. As an initial step towards the precision spectroscopic measurement of these transitions with an XUV frequency comb, an estimation was made by Herrman *et al.* using He^+ as a prototype system.[23] It was found that with an average power of $P = 10\,\mu$W in a single harmonic, focused down to $\omega_0 = 0.5\,\mu$m, the $1S$–$2S$ excitation is accessible and a detection rate of a few Hz can be reached. Thus, building an XUV frequency comb with more than 10 μW average power is an important step towards the bound state QED test experiment with improved precision.

In this work, we demonstrate the generation of an XUV frequency comb based on intracavity high harmonic generation (HHG) processes and the system can generate as much as 115.9 μW average power at ∼94 nm. The shortest wavelength of ∼55 nm has been reached with this system. The coherence of the generated light is tested with an optical-heterodyne-based measurement of the third harmonic. We also demonstrate that this setup can be used to study strong field physics with below threshold harmonics in molecular systems. These results suggest that the current system is ready for measuring narrow transitions in few-body systems, and ultimately, to improve the precision of QED test experiments as well as studying of strong field physics.

Figure 1 schematically shows our experimental setup. In our system, an Yb-doped fiber comb (Activefiber systems) is utilized for the driving laser. It delivers pulses with a repetition rate of 100 MHz, a central wavelength of 1038 nm, and a maximum output pulse energy of 1 μJ. Obviously, this pulse energy is too low to drive HHG process. Thus, we use a passive optical cavity to enhance the pulse energy of the pump laser. The detail of our femtosecond enhancement cavity (fsEC) has been described in Ref. [26]. Here, only a brief summary is given. The fsEC is a seven-mirror bowtie cavity, which is composed of an input coupler (IC) with $R = 99.2\%$, five high reflection mirrors with $R = 99.95\%$ and a diffraction nanograting which is etched directly on the top layer of a square

Supported by the National Natural Science Foundation of China (Grant Nos. 11674356 and 11527807), and the Strategic Priority Research Program of the Chinese Academy of Sciences (Grant No. XDB21010400).
*Corresponding author. Email: hualq@wipm.ac.cn; xjliu@wipm.ac.cn

high reflection mirror. The nanograting is designed to have an incidence angle of 70°, a grating period of 420 nm, a step height of 40 nm, and a duty cycle of 40%. With this design, the nanograting acts as a mirror with high reflectivity in the infrared (IR) region, thus it induces negligible reduction of the cavity finesse and power enhancement. While in XUV region, it acts as a grating and couples the generated HHG out of the cavity. The theoretical finesse and buildup of the cavity is about 600 and 290, respectively. By the aid of the Pound–Drever–Hall (PDH) technique,[27] the cavity length is locked to maintain the maximum intra-cavity power.[26] With a pump power of 24 W, we have achieved an intra-cavity power of 4.5 kW, and the corresponding buildup is about 188. The pulse duration is measured to be ∼330 fs by a frequency-resolved optical gating (FROG). The focus radius inside the cavity is estimated to be 8 μm (vertical) ×16 μm (horizontal) from an ABCD matrix analysis of the cavity. The peak intensity in the focus region is evaluated to be 3.3×10^{13} W/cm^2.

Xenon gas is delivered to the focus of the cavity by a quartz gas nozzle with a 1-bar backing pressure. The nozzle has a 150 μm wide opening and is installed on a 3-D translation stage, so that it can be precisely optimized to maximize the harmonic signal. A gas dump, connected to a dry pump, is installed right below the nozzle. It is beneficial to decrease the background pressure and to mitigate the absorption of the XUV light inside the chamber. A gas flow meter is utilized to control the gas pressure in the nozzle and the gas flow rate is typically 35 standard cubic centimeter per minute (sccm). The background pressure of the vacuum chamber is ∼0.54 Pa.

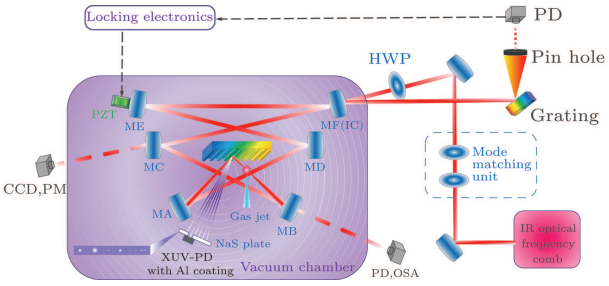

Fig. 1. Schematic view of the intracavity high harmonic generation. In the setup, the generated HHGs at the focus are out coupled by a nanograting, and thereafter imaged onto the NaS plate. The power of a specific harmonic is measured by an XUV diode which is mounted behind the NaS plate. PZT: piezo transducer, CCD: charge coupled device, PM: powermeter, PD: photodiode, OSA: optical spectrum analyzer, NaS plate: sodium salicylate plate, IC: input coupler, HWP: half wave plate, MA–MF: mirror A–mirror F.

We have measured the spectra and power of the high order harmonics that out coupled from the enhancement cavity. The harmonics are imaged onto a sodium salicylate fluorescent plate. Sodium salicylate generates fluorescent emission centered at 420 nm when excited by XUV light. It has a high fluorescent quantum yield and its response is independent of wavelength over the range from 30 nm to 100 nm.[28] Figure 2(a) shows the typical recorded image of produced HHGs on the fluorescent plate. The discrete harmonics produce individual spots on the fluorescent screen. The obtained two-dimensional images were integrated over the vertical direction to yield one-dimensional spectra of the out coupled harmonic radiation. The assignment of each measured harmonic order is shown in Fig. 2(b), and it is verified by the grating diffraction equation.

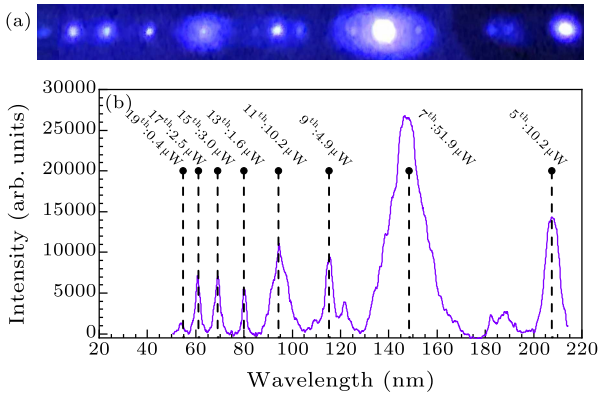

Fig. 2. (a) Image of the experimentally observed high order harmonics fluorescing on a plate coated with sodium salicylate. (b) The spectra of the out coupled high harmonic radiation obtained from the images of the fluorescent plate. The black dots and their drop-down lines indicate the wavelengths of the first order diffraction. Some peaks around 120 nm and 190 nm, which are not assigned in the figure, are the second/third order diffraction of the generated harmonics.

The power of the harmonics is measured with an XUV-sensitive silicon photodiode (AXUV100Al from Opto Diode Corp.). The photodiode has a 150-nm-thick aluminum filter in front of it to suppress the fundamental light at 1038 nm by more than 5 orders of magnitude. It can be used to directly measure the average power of the generated harmonics below 80 nm. A 1-mm-thick sodium salicylate plate with a 2-mm-width slit in the middle is pasted in front of the photodiode to make sure the target harmonic illuminates on the photodiode while the adjacent harmonic orders are still observable on the sodium salicylate plate. Both of the photodiode and the sodium salicylate plate are placed on a translation stage to ensure the specific harmonic order under measurement is at the optimized position. The average power of the 17th harmonic (∼61 nm) is measured to be 2.5 μW. The remaining harmonics is calculated based on the relative integrated power levels from the spectra, as shown in Fig. 2(b). In the XUV region, the 11th harmonic (∼94 nm) has the highest average power, i.e., 10.2 μW. The efficiency of the grating at this wavelength is calculated to be about 8.8% by the aid of rigorous coupled wave analysis (RCWA).[29,30] Thus,

the generated average power of the 11th harmonic is estimated to be 115.9 μW. The intracavity conversion efficiency is $\sim 2.5 \times 10^{-8}$. The efficiency of the grating at 7th harmonic (~148 nm) is calculated to be 4.0%, corresponding to 1.3 mW average power generated for the 7th harmonic. A relative higher conversion efficiency, i.e., $\sim 2.9 \times 10^{-7}$, is reached at this wavelength.

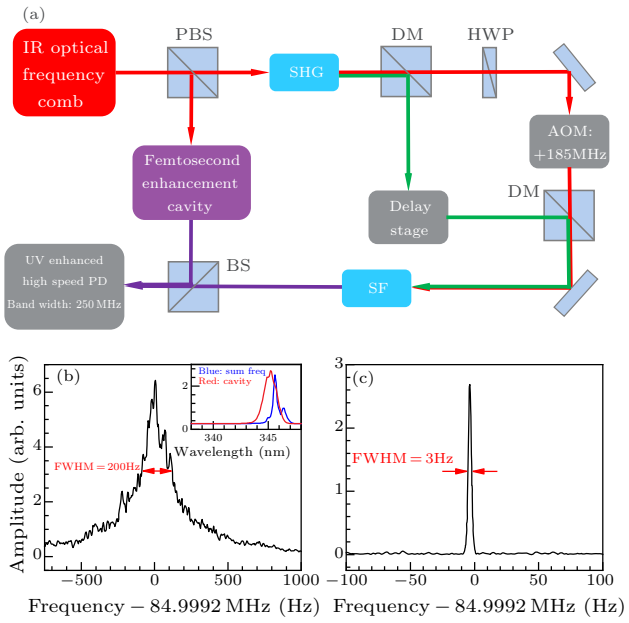

Fig. 3. (a) Schematic diagram for the optical heterodyne beat measurement. PBS: polarization beam splitter, DM: dichromatic mirror, HWP: half wave plate, BS: beam splitter, SHG: second harmonic generation, SF: sum frequency. (b) The beat signal before locking the phase of the interferometer. Inset: spectra of the third harmonic from the fsEC and the sum frequency generation process. (c) The linewidth of the beat signal decreases to ~3 Hz (1 Hz resolution bandwidth) after locking the phase of the interferometer.

Next, we proceed to investigate the temporal coherence properties of the harmonic generated inside the fsEC by an optical heterodyne beating experiment. The infrared optical comb is split into two beams by a polarization beam splitter. One beam is injected into the fsEC for intra-cavity HHG process, while the other is used for sum frequency generation using its second harmonic and its fundamental radiation. Two generated third harmonics (H3) are then combined together to detect the heterodyne beat between them. The schematic of the experimental setup is shown in Fig. 3(a). A 185 MHz acousto-optic modulator (AOM) is inserted into one of the interferometer arm so that the beat detection is shifted to a convenient nonzero frequency. By optimizing the temporal and spatial overlap of the two H3 beams, the beat signal can be obtained. We note that the spectra of the H3 generated by the sum frequency generation process are sensitive to the orientation of the nonlinear crystals, and the spectra of H3 generated inside the fsEC are sensitive to the fundamental comb spectra that are enhanced in the cavity. Thus, it is important to optimize the spectral overlap of the two H3 beams [shown in the upper right of Fig. 3(b)] to maximize the intensity of the beat signal. The full width of half maximum (FWHM) of the beat signal is about 200 Hz, as shown in Fig. 3(b). This linewidth is affected largely by the path length fluctuations of the two arms of the interferometer. To lock the path length, i.e., the phase of the interferometer, the AOM is modulated with a rate of 10 kHz/V in one arm. The beat signal is filtered and mixed with an 84.9992-MHz local signal. The output is then processed by the proportional-integral-derivative (PID) circuit and fed back to the modulation of the AOM. After locking the path length, the linewidth is reduced to ~3 Hz with 1 Hz resolution bandwidth (RBW) of our fast Fourier transform (FFT) spectrometer, as shown in Fig. 3(c). This indicates that the coherence time of our XUV frequency comb has the potential to reach a few milliseconds once the driving IR comb can be ultimately controlled.

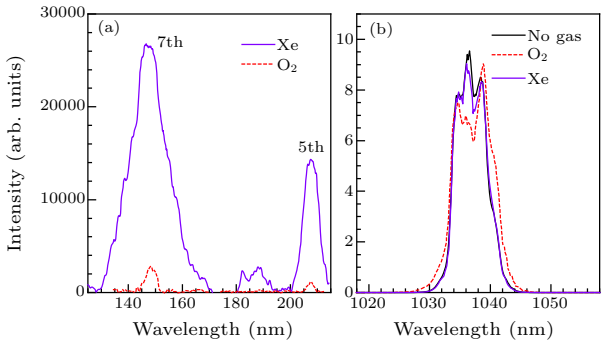

Fig. 4. (a) The spectra of the outcoupled high harmonic radiation for xenon and oxygen. (b) The intracavity transmitted IR spectra for no gas, xenon and oxygen.

Lastly, we demonstrate that the current setup also provides a powerful platform to study the strong field physics with the aid of intra-cavity HHG at an unprecedented high repetition rate of 100 MHz. Compared to typical strong field physics experiments with Ti:sapphire amplifier at 1 kHz, this represents an increase of about 5 orders of magnitude in the repetition rate, thus providing an improved precision and a more comprehensive understanding of the interaction of the strong field with atoms and molecules.[13] Under identical laser condition, we have measured and compared the HHG spectra both from Xe and O_2. Both species have similar ionization potentials (~12.1 eV), but with different ground state electronic structure. A strong suppression of the HHG is observed in the case of O_2, as shown in Fig. 4(a). The average power of the 5th and the 7th harmonics are measured to be only 0.4 μW and 2.3 μW, respectively. Note that a strong suppression of the harmonics generation in O_2 in the plateau region has been studied before[31,32] and can be well understood by the two-atomic-center interference effect on strong field tunnel ionization of molecular O_2.[33] The current study reveals that the

suppression also exists for below threshold harmonics, where multiphoton processes are believed to dominate, especially in the case of the 5th harmonics.[4] Moreover, an obvious spectral broadening of the driving IR comb is observed in the case of O_2, as shown in Fig. 4(b). This spectral broadening is due to the impulsive stimulated Raman excitation of the rotational states of the O_2 molecules, as in the case of N_2O.[13] A dip around 1037 nm is also observed, and it is likely due to the phase shift that is induced by the impulsive stimulated Raman excitation process. This phase shift modulates the enhancement factors of different comb modes. One should note that this spectra change has not been observed and been ignored under the case of 1 kHz driving laser with a thin gas jet. However, in the current system which works at 100 MHz, the fsEC increases the interaction length between the laser and the molecules by a factor proportional to the cavity finesse, thus providing an improved precision of measuring the interaction of the strong field with atoms and molecules.

In conclusion, we have built an XUV frequency comb system that provides as much as 115.9 μW (1.3 mW) average power at ∼94 nm (∼148 nm) through high harmonic generation. The shortest wavelength we can reach is ∼55 nm. The beat signal of the third harmonic shows a linewidth of ∼3 Hz, indicating that the coherence time of our XUV frequency comb has the potential to reach a few milliseconds once the driving IR comb can be ultimately controlled. With this system, we also observe a suppression of the harmonics yield in O_2 compared to that of Xe under the same laser condition, revealing that the suppression of harmonics generation also exists in below threshold harmonics, where multiphoton processes are believed to play an important role. This newly established XUV frequency comb system in our lab provides a versatile platform for the studies in precision spectroscopy measurements and strong field physics with an unprecedented repetition rate of 100 MHz.

We thank Professor Jinlong Zhang and Professor Zhanshan Wang at Tongji University for manufacturing the nanograting.

References

[1] Jones R J, Moll K D, Thorpe M J and Ye J 2005 *Phys. Rev. Lett.* **94** 193201

[2] Gohle C, Udem T, Herrmann M, Rauschenberger J, Holzwarth R, Schuessler H A, Krausz F and Hänsch T W 2005 *Nature* **436** 234

[3] Ozawa A, Rauschenberger J, Gohle C, Herrmann M, Walker D R, P V, Fernandez A, Graf R, Apolonski A, Holzwarth R, Krausz F, Hänsch T W and Udem T 2008 *Phys. Rev. Lett.* **100** 253901

[4] Yost D C, Schibli T R, Ye J, Tate J L, Hostetter J, Gaarde M B and Schafer K J 2009 *Nat. Phys.* **5** 815

[5] Pronin O, Pervak V, Fill E, Rauschenberger J, Krausz F and Apolonski A 2011 *Opt. Express* **19** 10232

[6] Yang Y Y, Süßmann F, Zherebtsov S, Pupeza I, Kaster J, Lehr D, Fuchs H J, Kley E B, Fill E, Duan X M, Zhao Z S, Krausz F, Stebbings S L and Kling M F 2011 *Opt. Express* **19** 1954

[7] Lee J, Carlson D R and Jones R J 2011 *Opt. Express* **19** 23315

[8] Cingöz A, Yost D C, Allison T K, Ruehl A, Fermann M E, Hartl I and Ye J 2012 *Nature* **482** 68

[9] Mills A K, Hammond T J, Lam M H C and Jones D J 2012 *J. Phys. B: At. Mol. Opt. Phys.* **45** 142001

[10] Pupeza I, Holzberger S, Eidam T, Carstens H, Esser D, Weitenberg J, Russbuldt P, Rauschenberger J, Limpert J, Udem T, Tünnermann A, Hänsch T W, Apolonski A, Krausz F and Fill E 2013 *Nat. Photon.* **7** 608

[11] Pupeza I, Högner M, Weitenberg J, Holzberger S, Esser D, Eidam T, Limpert J, Tünnermann A, Fill E and Yakovlev V S 2014 *Phys. Rev. Lett.* **112** 103902

[12] Benko C, Allison T K, Cingoz A, Hua L, Labaye F, Yost D C and Ye J 2014 *Nat. Photon.* **8** 530

[13] Benko C, Hua L, Allison T K, Labaye F and Ye J 2015 *Phys. Rev. Lett.* **114** 153001

[14] Holzberger S, Lilienfein N, Carstens H, Saule T, Högner M, Lücking F, Trubetskov M, P V, Eidam T, Limpert J, Tünnermann A, Fill E, Krausz F and Pupeza I 2015 *Phys. Rev. Lett.* **115** 023902

[15] Porat G, Heyl C M, Schoun S B, Benko C, Dorre N, Corwin K L and Ye J 2018 *Nat. Photon.* **12** 387

[16] Seres J, Seres E, Serrat C, Young E C, Speck J S and Schumm T 2019 *Opt. Express* **27** 6618

[17] Ozawa A and Kobayashi Y 2013 *Phys. Rev. A* **87** 022507

[18] Högner M, T V and Pupeza I 2017 *New J. Phys.* **19** 033040

[19] Zheng X, Sun Y R, Chen J and Hu S 2018 *Acta Phys. Sin.* **67** 164203 (in Chinese)

[20] Eyler E E, Chieda D E, Stowe M C, Thorpe M J, Schibli T R and Ye J 2008 *Eur. Phys. J. D* **48** 43

[21] Bergeson S D, Balakrishnan A, Baldwin K G H, Lucatorto T B, Marangos J P, McIlrath T J, O'Brian T R, Rolston S L, Sansonetti C J, Wen J, Westbrook N, Cheng C H and Eyler E E 1998 *Phys. Rev. Lett.* **80** 3475

[22] Haas M, Jentschura U D, Keitel C H, Kolachevsky N, Herrmann M, Fendel P, Fischer M, Udem T, Holzwarth R, Hänsch T W, Scully M O and Agarwal G S 2006 *Phys. Rev. A* **73** 052501

[23] Herrmann M, Haas M, Jentschura U D, Kottmann F, Leibfried D, Saathoff G, Gohle C, Ozawa A, B V, Knunz S, Kolachevsky N, Schussler H A, Hänsch T W and Udem T 2009 *Phys. Rev. A* **79** 052505

[24] Prior M H and Shugart H A 1971 *Phys. Rev. Lett.* **27** 902

[25] Semczuk M 2009 *An Ion Trap for Laser Spectroscopy on Lithium Ions* MS Thesis (Warsaw: University of Warsaw)

[26] Zhang J, Hua L Q, Yu S G, Chen Z and Liu X J 2019 *Chin. Phys. B* **28** 044206

[27] Black E D 2001 *Am. J. Phys.* **69** 79

[28] Publications J A R 1967 *Techniques in Vacuum Ultraviolet Spectroscopy* (PIED Publications)

[29] Moharam M G, Grann E B and Pommet D A 1995 *J. Opt. Soc. Am. A* **12** 1068

[30] Moharam M G, Pommet D A and Grann E B 1995 *J. Opt. Soc. Am. A* **12** 1077

[31] Li G H, Yao J P, Zhang H S, Jing C R, Zeng B, Chu W, Ni J L, Xie H Q, Liu X J, Chen J, Cheng Y and Xu Z Z 2013 *Phys. Rev. A* **88** 043401

[32] Shan B, Tong X M, Zhao Z X, Chang Z H and Lin C D 2002 *Phys. Rev. A* **66** 061401

[33] Lin Z Y, Jia X Y, Wang C L, Hu Z L, Kang H P, Quan W, Lai X Y, Liu X J, Chen J, Zeng B, Chu W, Yao J P, Cheng Y and Xu Z Z 2012 *Phys. Rev. Lett.* **108** 223001